

# First Observation of Multiple Transverse Wobbling Bands of Different Kinds in $^{183}\text{Au}$

S. Nandi<sup>1,2</sup>, G. Mukherjee<sup>1,2</sup>, Q. B. Chen<sup>3</sup>, S. Frauendorf<sup>4</sup>, R. Banik<sup>1,2</sup>, Soumik Bhattacharya<sup>1,2</sup>, Shabir Dar<sup>1,2</sup>, S. Bhattacharyya<sup>1,2</sup>, C. Bhattacharya<sup>1,2</sup>, S. Chatterjee<sup>5</sup>, S. Das<sup>5</sup>, S. Samanta<sup>5</sup>, R. Raut<sup>5</sup>, S.S. Ghugre<sup>5</sup>, S. Rajbanshi<sup>6</sup>, Sajad Ali<sup>7</sup>, H. Pai<sup>8</sup>, Md. A. Asgar<sup>9</sup>, S. Das Gupta<sup>10</sup>, P. Chowdhury<sup>11</sup>, A. Goswami<sup>8</sup>

<sup>1</sup>Variable Energy Cyclotron Centre, 1/AF, Bidhan Nagar, Kolkata - 700064, India

<sup>2</sup>Homi Bhabha National Institute, Training School Complex, Anushakti Nagar, Mumnaï - 400094, India

<sup>3</sup>Physik-Department, Technische Universität München, D-85747 Garching, Germany

<sup>4</sup>Department of Physics, University of Notre Dame, Notre Dame, Indiana 46556, USA

<sup>5</sup>UGC-DAE CSR, Kolkata Centre, Kolkata 700098, India

<sup>6</sup>Department of Physics, Presidency University, Kolkata 700043, India

<sup>7</sup>Government General Degree College at Pedong, Kalimpong 734311, India

<sup>8</sup>Saha Institute of Nuclear Physics, Kolkata 700064, India

<sup>9</sup>Department of Physics, Prabhat Kumar College, Contai 721404, India

<sup>10</sup>Victoria Institution (College), Kolkata 700009, India and

<sup>11</sup>University of Massachusetts Lowell, Lowell MA 01854, USA

(Dated: September 2, 2020)

We report the first observation of two wobbling bands in  $^{183}\text{Au}$ , both of which were interpreted as the transverse wobbling (TW) band but with different behavior of their wobbling energies as a function of spin. It increases (decreases) with spin for the positive (negative) parity configuration. The crucial evidence for the wobbling nature of the bands, dominance of the  $E2$  component in the  $\Delta I = 1$  transitions between the partner bands, is provided by the simultaneous measurements of directional correlation from the oriented states (DCO) ratio and the linear polarization of the  $\gamma$  rays. Particle rotor model calculations with triaxial deformation reproduce the experimental data well. A value of spin,  $I_m$ , has been determined for the observed TW bands below which the wobbling energy increases and above which it decreases with spin. The nucleus  $^{183}\text{Au}$  is, so far, the only nucleus in which both the increasing and the decreasing parts are observed and thus gives the experimental evidence of the complete transverse wobbling phenomenon.

Nuclear wobbling excitation is a manifestation of non-axial nuclear shape which was first discussed by Bohr and Mottelson [1]. The non-axial (triaxial) nuclear shape appears due to the unequal nuclear mass distribution along the three principal axes and implies three unequal moments of inertia about the three principal axes. A triaxially deformed nucleus always tries to rotate around the medium ( $m$ ) axis having the largest moment of inertia but the presence of the rotations around the other two axes i.e., short ( $s$ ) and long ( $l$ ), generates a precession of the medium axis rotation about the space-fixed angular momentum axis, similar to the classical wobbling motion of an asymmetric top [2]. The energy spectrum of this excitation is given by [1]:

$$E = E_{\text{rot}} + (n_w + 1/2)\hbar\omega_{\text{wob}}$$

where, the term  $E_{\text{rot}}$ , corresponds to the rotation about the medium axis while  $n_w$  is the wobbling quanta and  $\hbar\omega_{\text{wob}}$  is the wobbling frequency with wobbling energy  $E_{\text{wob}} = \hbar\omega_{\text{wob}}$ . This generates a series of rotational bands with different  $n_w$ .

This exotic excitation has been observed only in a few odd- $A$  nuclei [3–13]. In case of the odd- $A$  nuclei, the odd particle in high- $j$  orbital couples with a triaxial core and modifies the wobbling motion. Depending on the coupling of the odd particle, two types of wobbling bands can be observed: Longitudinal Wobbling (LW) and Transverse Wobbling (TW) [14]. In LW, the angular momentum of the odd particle aligns along the medium axis

while in TW, it aligns along one of the perpendicular axes (short or long).

An extensive theoretical description of the wobbling motion has been given by Frauendorf and Dönau [14] in terms of a quasiparticle triaxial rotor (QTR) model. Analytical expression for  $\hbar\omega_{\text{wob}}$  has been derived with the assumption of “Frozen Alignment” and harmonic oscillation (HFA). It was shown that  $E_{\text{wob}}$  increases as a function of angular momentum ( $I$ ) in case of LW which has been recently observed experimentally in  $^{133}\text{La}$  [10] and  $^{187}\text{Au}$  [12]. However, in case of TW, the variation of  $E_{\text{wob}}$  is highly dependent on the values of the moments of inertia,  $\mathcal{J}_m$ ,  $\mathcal{J}_s$  and  $\mathcal{J}_l$  along the medium, short and long axes, respectively, of the triaxial core. In general,  $E_{\text{wob}}$  decreases with  $I$ . But in a situation where  $\mathcal{J}_m$  is slightly larger than  $\mathcal{J}_s$  and both are much larger than  $\mathcal{J}_l$ , the value of  $E_{\text{wob}}$  increases with the increase of  $I$  for the lower values of  $I$  and then decreases with  $I$  [14]. So far, in all the cases, in which the experimental evidence of TW bands have been reported, only the decreasing part of the  $E_{\text{wob}}$  has been observed. Therefore, it was generally believed that the LW and TW can be distinguished from the variation of  $E_{\text{wob}}$  with  $I$ ; increasing (decreasing) of which corresponds to LW (TW).

In this letter we report the observation of two TW bands in  $^{183}\text{Au}$ .  $E_{\text{wob}}$  has been found to increase with  $I$  in one of these bands, the first example of such a behavior of a TW band, while in the other band  $E_{\text{wob}}$  decreases with  $I$ . Thereby, it constitutes the only example of experimental observation of a complete scenario of the

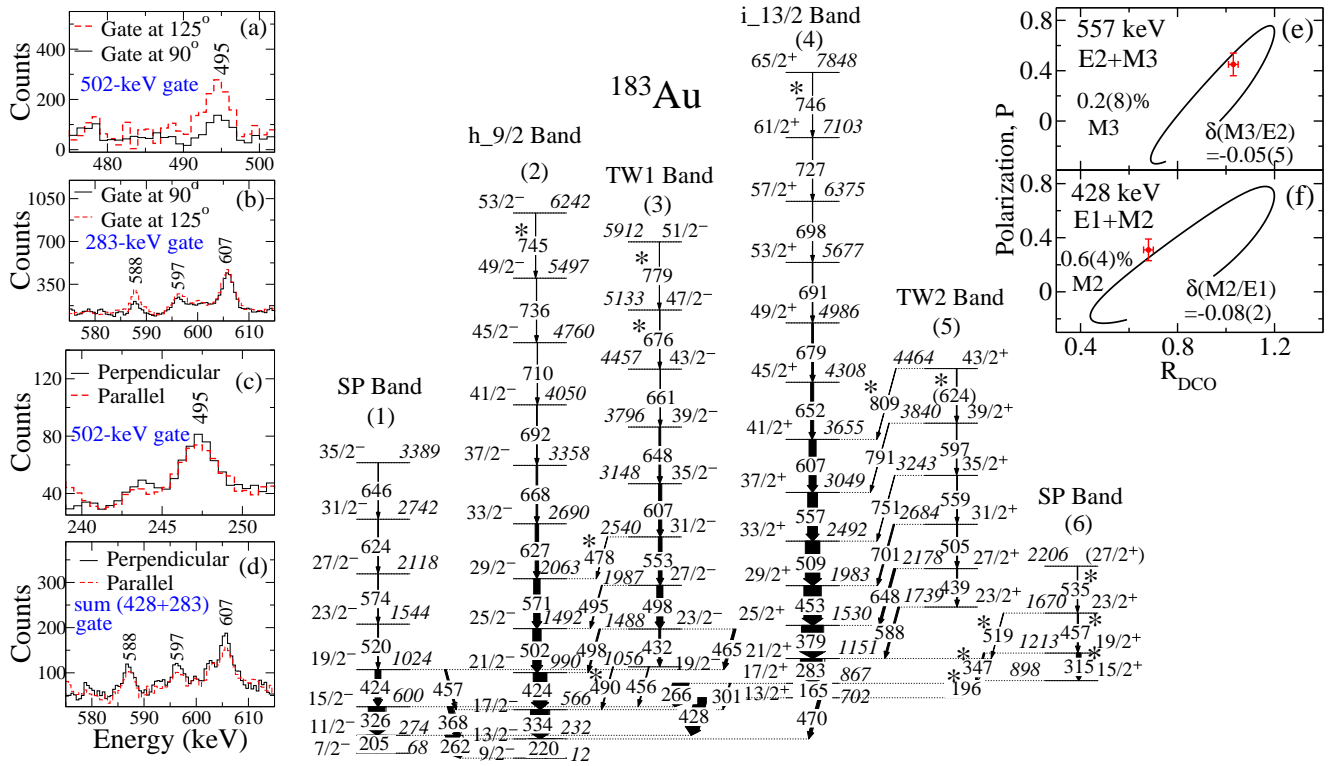


FIG. 1. Level scheme of  $^{183}\text{Au}$ , established from the present work. Line widths are proportional to their intensities. The level energies are obtained by fitting the  $\gamma$ -ray energies using the code *GTOL* [15]. Representative gated  $\gamma$ -ray spectra for a few transitions, projected from the 2-dimensional DCO and polarization matrices, are shown in the insets (a), (b) (c) and (d). The spectra in (a) and (b) are used for DCO ratio ( $R_{DCO}$ ) whereas (c) and (d) are used for linear polarization ( $P$ ) measurements. The insets (e) and (f) show the experimental (symbol) and calculated (solid line) values of  $R_{DCO}$  and  $P$  of two of the transitions in  $^{183}\text{Au}$ . The 557 keV is a known  $E2$  transition decaying from  $37/2^+$  to  $33/2^+$  in band (4) and 428 keV is a known  $E1$  transition from  $13/2^+$  to  $11/2^-$  between band (4) and band (1). These transitions show very small mixing ratios ( $\delta$ ) as they should be. The new transitions in the level scheme are marked by asterisks.

transverse wobbling phenomenon.

The excited  $n_w = 1$  wobbling bands decay to the  $n_w = 0$  yrast bands via  $\Delta I = 1$ , collectively enhanced  $E2$  transitions [12, 14]. On the other hand, in case of the signature partner (SP) bands (which occurs when the odd-particle angular momentum is not fully aligned with the rotation axis), the connecting transitions are predominantly  $\Delta I = 1$ ,  $M1$  type [12]. Therefore, experimentally the wobbling partner band and the SP band can be distinguished from the nature of the connecting transitions between the partner band and the yrast band. For clear identification of wobbling, it is important to experimentally observe both the signature partner band and the wobbling partner band decaying to the main band.

The excited states of  $^{183}\text{Au}$  in this work were populated using the  $^{169}\text{Tm}(^{20}\text{Ne}, 6n)^{183}\text{Au}$  fusion evaporation reaction at the bombarding energy of 146-MeV from the K-130 cyclotron facility at the Variable Energy Cyclotron Centre (VECC), Kolkata. A thick ( $23 \text{ mg/cm}^2$ )  $^{169}\text{Tm}$  foil was used as the target for this experiment. The  $\gamma$  rays emitted from the residual nuclei were detected by the Indian National Gamma Array (*INGA*) facility which

was composed of eight Compton-suppressed (BGO anti-Compton shields) clover HPGe detectors and two HPGe planar LEPS (Low Energy Photon Spectrometer). A total of  $1.5 \times 10^9$  two- and higher-fold coincidence data with time stamp were recorded in a fast (250 MHz) digital data acquisition system based on Pixie-16 modules of XIA [16]. The data were sorted using the IUCPIX package [16], and were analyzed using the radware package [17]. Several  $E_\gamma$ - $E_\gamma$  coincidence matrices and a  $E_\gamma$ - $E_\gamma$ - $E_\gamma$  cube were constructed from which single- and double-gated spectra were projected for the analysis.

A new and improved level scheme of  $^{183}\text{Au}$  has been established (Fig. 1) with 14 new  $\gamma$  rays including a new band, the band (6), compared to the previous studies [18, 19]. Representative gated spectra are shown in the insets in Fig. 1.

For unambiguous assignment of multipolarity ( $\lambda$ ) and type ( $E/M$ ) of a  $\gamma$ -ray transition as well as its mixing ratio  $\delta$ , in case of a mixed transition (e.g.  $M1 + E2$ ), the combined measurements of linear polarization ( $P$ ) and DCO (Directional Correlation from the Oriented states) ratio ( $R_{DCO}$ ), as described in Ref. [20–24], have been

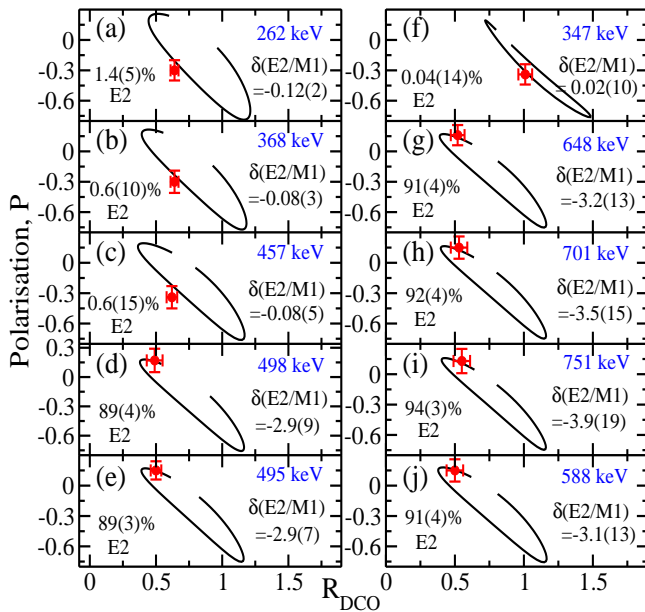


FIG. 2. Experimental (symbol) and calculated (solid line) values (for different mixing ratios  $\delta$ ) of DCO ratios ( $R_{DCO}$ ) and linear polarization ( $P$ ) of the connecting transitions that decay to the negative parity band (2) (a – e) and to the positive parity band (4) (f – j).

performed. The measured values of  $P$  and  $R_{DCO}$  of a  $\gamma$  ray have been compared with the values calculated for several  $\delta$ . For a pure transition, the measured values would lie close to the ones calculated with  $\delta \sim 0$ . This is demonstrated for two transitions in  $^{183}\text{Au}$ , known to be E2 and E1 (see insets (b) and (c) of Fig. 1). In the case of  $\Delta I = 1$  transition with enhanced E2 component, measured values would lie close to the calculated ones with large  $\delta$ .

Both negative- and positive-parity yrast bands, band (2) and (4), in  $^{183}\text{Au}$  have two side bands each and are connected by  $\Delta I = 1$  transitions. The measured and the calculated values of  $P$  and  $R_{DCO}$  for these connecting transitions are plotted in Fig. 2. The low values of  $\delta$ , obtained for the connecting transitions from bands (1) and (6) to the respective negative and positive parity yrast bands, suggest that they are mostly of pure M1 type (about 1% E2). On the other hand, quite large values of  $\delta$  are resulted for the transitions connecting the side bands (3) and (5) to the respective yrast bands, It clearly indicates the predominantly E2 nature (about 90% E2) of these transitions. Therefore, the bands (1) and (6) have been identified as the SP bands, while the bands (3) and (5) are identified as the one-phonon wobbling ( $n_w = 1$ ) bands. It is the first instance that a pair of wobbling bands with positive and negative parity has been identified in a nucleus.

The positive and the negative parity bands in  $^{183}\text{Au}$  were assigned the configurations  $\pi i_{13/2}$  and  $\pi h_{9/2}$ , respectively [19]. Both of these orbitals are situated above

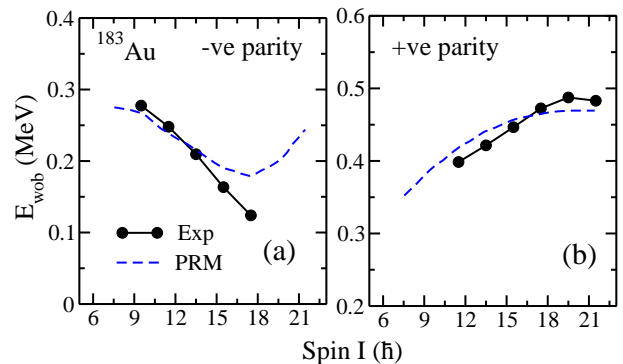


FIG. 3. Experimental wobbling energy  $E_{wob}$  as a function of angular momentum  $I$  for the negative parity (a) and the positive parity (b) bands in  $^{183}\text{Au}$ . The theoretically calculated values are also shown. The error bars on experimental values are within the size of the data points.

the  $Z = 82$  shell closure and, hence, they are of particle character with large contribution from the low- $\Omega$  ( $\Omega =$  projection of the particle angular momentum on to the symmetry axis) Nilsson configuration. The quasiparticle aligned angular momentum  $i_x \approx 6.5\hbar$ , estimated for the positive parity yrast band from its level energies, indicates fully aligned  $\Omega = 1/2$ ,  $i_{13/2}$  configuration. In case of the negative parity band, the estimated value of  $i_x$  ( $\approx 3.5\hbar$ ) is somewhat less than the fully aligned value ( $= 4.5\hbar$ ), suggesting a small mixing with larger  $\Omega$  orbitals. However, both of these situations favor the alignment of the odd particle perpendicular to the medium axis and, hence, the occurrence of transverse wobbling.

It was shown in Ref. [14] that the variation of the wobbling energy with spin ( $I$ ) depends on the type (LW or TW) of wobbling motion. Experimentally, the wobbling energy  $E_{wob} = \hbar\omega_{wob}$  can be obtained from the energy differences between the  $n_w = 1$  wobbling partner band and  $n_w = 0$  yrast band using the relation [9–12]

$$E_{wob} = E(I, n_w = 1) - [E(I - 1, n_w = 0) + E(I + 1, n_w = 0)]/2,$$

where  $E(I)$  is the excitation energy of the state with angular momentum  $I$ .

The experimental values of  $E_{wob}$  for both the wobbling bands, identified in  $^{183}\text{Au}$  in the present work, are plotted in Fig. 3. It can be seen that the wobbling energy decreases (increases) with  $I$  for the negative (positive) parity band and hence, it may be, in general, considered as TW (LW). However, the low- $\Omega$ ,  $i_{13/2}$  configuration for the positive parity band is in contradiction to the LW geometry of the coupling of the odd quasiparticle. Therefore, this band is, most likely, the initial part of a TW band, predicted in Ref.[14] for the same  $\pi i_{13/2}$  configuration in  $^{163}\text{Lu}$  but has not been observed in any nucleus prior to this work.

In order to understand the observation of wobbling bands in  $^{183}\text{Au}$ , theoretical calculations in the frame work

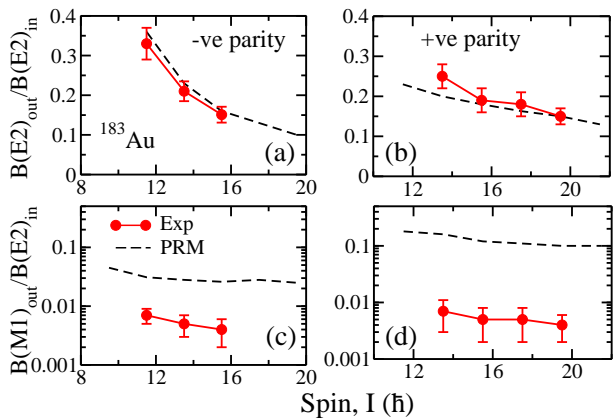


FIG. 4. Measured values of the ratio of transition probabilities,  $B(E2)_{\text{out}}/B(E2)_{\text{in}}$  and  $B(M1)_{\text{out}}/B(E2)_{\text{in}}$ , determined from the  $\gamma$ -ray intensities, as a function of angular momentum  $I$  for the negative parity (a and c) and the positive parity (b and d) bands in  $^{183}\text{Au}$ . The theoretical values calculated from PRM are also shown.

of particle rotor model (PRM) [14, 25–28] has been performed. As the input to the calculations, the deformation parameters of  $\beta = 0.30$  and  $\gamma = 20.0^\circ$  and the moments of inertia  $\mathcal{J}_{m,s,l} = 36.85, 25.70, 5.45 \hbar^2/\text{MeV}$  for the negative parity band, while  $\beta = 0.29$ ,  $\gamma = 21.4^\circ$ , and  $\mathcal{J}_{m,s,l} = 50.00, 37.52, 2.38 \hbar^2/\text{MeV}$  for the positive parity band have been used. The deformation parameters are obtained by the covariant density functional theory (CDFT) [29, 30] with PC-PK1 effective interaction [31], and the moments of inertia are fitted to the energy spectra. In both calculations, the pairing gap  $\Delta = 12/\sqrt{A} = 0.89 \text{ MeV}$  is adopted. It should be noted that the calculations can reproduce the experimental  $B(E2)$  values [32], which justifies the correct prediction of the deformation parameters by CDFT. We have also carried out calculations by including cranking terms. The equilibrium deformations for both negative and positive parity bands change only within 0.01 for  $\beta$  and  $1^\circ$  for  $\gamma$  from the bandhead to the highest spin, which justifies the assumption of a constant deformation for the PRM calculations.

The results of the calculations are shown in Figs. 3 and 4. The wobbling energies ( $E_{\text{wob}}$ ) for both the bands are well reproduced in the calculations. Moreover, the experimental  $B(E2)_{\text{out}}/B(E2)_{\text{in}}$  values, determined from the measured  $\gamma$ -ray intensities, agree well with the calculated ones (Fig. 4) which justifies the correct inputs of triaxiality by CDFT. The overestimation of the  $B(M1)_{\text{out}}/B(E2)_{\text{in}}$  values is attributed to the absence of scissors mode in the calculations [33]. The large  $B(E2)_{\text{out}}/B(E2)_{\text{in}}$  and small  $B(M1)_{\text{out}}/B(E2)_{\text{in}}$  values further support the wobbling interpretation for both the bands.

The values of the three moments of inertia obtained for the two wobbling bands in  $^{183}\text{Au}$  indicate that the ratios

TABLE I. The moments of inertia along medium ( $\mathcal{J}_m$ ), short ( $\mathcal{J}_s$ ) and long ( $\mathcal{J}_l$ ) axes obtained for the wobbling bands in  $^{183}\text{Au}$ ,  $^{135}\text{Pr}$  and  $^{105}\text{Pd}$ . The values for the later two nuclei are taken from Ref. [14] and [9], respectively. The estimated values of  $I_m$  based on HFA approximation are also given.

	$^{183}\text{Au}$	$^{183}\text{Au}$	$^{135}\text{Pr}$	$^{105}\text{Pd}$
	$\pi i_{13/2}$ band	$\pi h_{9/2}$ band	$\pi h_{11/2}$ band	$\nu h_{11/2}$ band
$\mathcal{J}_m$	50.00	36.85	21.0	9.24
$\mathcal{J}_s$	37.52	25.70	13.0	5.87
$\mathcal{J}_l$	2.38	5.45	4.0	1.99
$\mathcal{J}_m/\mathcal{J}_s$	1.33	1.43	1.61	1.57
$I_m$ ( $\hbar$ )	16.5	7.5	5.5	6.5

of both  $\mathcal{J}_m/\mathcal{J}_l$  and  $\mathcal{J}_s/\mathcal{J}_l$  are much higher in case of the positive parity  $\pi i_{13/2}$  band. It makes this band an ideal candidate for the observation of the, hitherto unobserved, initial part of a TW band in which  $E_{\text{wob}}$  increases with  $I$  until a certain value  $I_m$  after which, it starts to decrease. The value of  $I_m$  must be sufficiently large in order to experimentally observe the increasing part. According to the harmonic wobbling model with frozen orbital approximation (HFA) of Ref. [14], the larger is the value of the quasi particle angular momentum  $j$ , and closer is the value of  $\mathcal{J}_m / \mathcal{J}_s$  to unity, the larger will be the value of  $I_m$ .

The  $I_m$  values estimated from the HFA model in  $^{183}\text{Au}$  have been compared, in Table I, with the TW bands reported in the two other normal deformed nuclei,  $^{105}\text{Pd}$  [9] and  $^{135}\text{Pr}$  [11]. The configurations of the TW bands in  $^{105}\text{Pd}$  and  $^{135}\text{Pr}$  are  $\nu h_{11/2}$  and  $\pi h_{11/2}$ , respectively. The value of  $I_m$  is the largest for the  $\pi i_{13/2}$  band in  $^{183}\text{Au}$  among these nuclei and is much more than the initial spin of its wobbling band. Therefore,  $E_{\text{wob}}$  for this band would fall in the increasing part of the predicted TW band. This is further established from Fig. 5 in which  $E_{\text{wob}}$  calculated from the HFA model using the fitted moments of inertia values  $\mathcal{J}_{m,s,l}$  from Table I are plotted as a function of spin along with the measured  $E_{\text{wob}}$ . The calculated values are suitably normalised for comparison. Excellent agreement between experiment and theory has been achieved for all the cases. It can be seen that the data points corresponding to the  $\pi i_{13/2}$  band in  $^{183}\text{Au}$  match with the increasing part while for the others they fall nicely on the decreasing part of the curves for which the values of  $I_m$  are lower than the lowest spin of the observed wobbling bands.

This shows, for the first time, an experimental evidence of the general nature of the TW bands in terms of the variation of the wobbling energy in which both increasing and decreasing parts of the  $E_{\text{wob}}$  are observed.

It may also be pointed out that similar to the multiple chiral doublet ( $M\chi D$ ) bands [30], the observation of the presence of multiple TW bands is also an evidence of triaxial shape coexistence in  $^{183}\text{Au}$ . Though the triaxial shape coexistence has been experimentally confirmed in several nuclei through  $M\chi D$  bands (see for

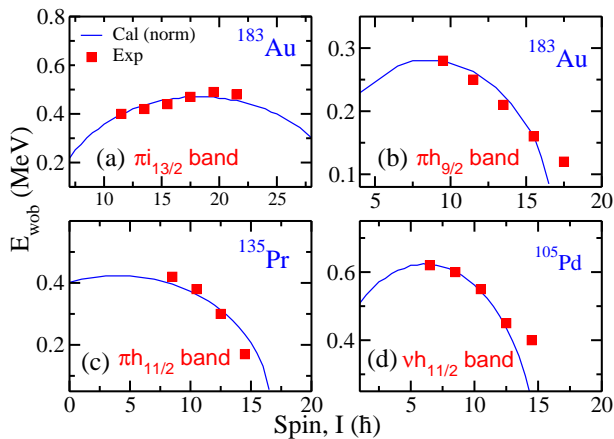


FIG. 5. Experimental and calculated values (see text for details) of wobbling energies as a function of angular momentum ( $I$ ) for the (a) positive ( $i_{13/2}$ ) and (b) negative ( $h_{9/2}$ ) parity wobbling bands in  $^{183}\text{Au}$ . For comparison, the same for the normal deformed TW bands in  $^{135}\text{Pr}$  (c) and  $^{105}\text{Pd}$  (d) are also shown. Data for the later two nuclei are obtained from Ref.[11] and [9], respectively.

example [34, 35] and references there in), but its realization through the observation of multiple wobbling bands is being reported for the first time.

In summary, clear experimental evidence for the existence of two wobbling bands, based on a positive ( $i_{13/2}$ ) and a negative ( $h_{9/2}$ ) parity configuration, has been observed in  $^{183}\text{Au}$ . Both the bands are suggested as the transverse wobbling bands based on the calculations by PRM and HFA models. The present work represents the first observation of TW bands in  $A \sim 180$  region and a first identification of the initial increasing part of wob-

bling energy as a function of spin in a TW band, in the whole of the nuclear chart. One important conclusion from the present work is that the decrease of  $E_{\text{wob}}$  with  $I$  may not be considered as a necessary condition for the evidence of TW. Moreover, this is, so far, the only example of the observation of wobbling bands based on both positive and negative parity configurations in a single nucleus and represents the first evidence of triaxial shape coexistence in Au isotopes.

## ACKNOWLEDGMENTS

The authors gratefully acknowledge the effort of the cyclotron operators at VECC, Kolkata for providing a good quality of  $^{20}\text{Ne}$  beam. We thank all the members of VECC INGA collaboration for setting up the array. Partial financial support from Department of Science & Technology (DST), Govt. of India is gratefully acknowledged for the clover detectors of INGA (Grant no No. IR/S2/PF-03/2003-II). SN, RB and S. Dar acknowledge with thanks the financial support received as research fellows from the Department of Atomic Energy (DAE), Govt. of India. HP acknowledges the support received from the Ramanujan Fellowship Research Grant under SERB-DST Grant No. SB/S2/RJN-031/2016 of Govt. of India. The work of Q. B. C. was supported by Deutsche Forschungsgemeinschaft (DFG) and National Natural Science Foundation of China (NSFC) through funds provided to the Sino-German CRC 110 ‘‘Symmetries and the Emergence of Structure in QCD’’ (DFG Grant No. TRR110 and NSFC Grant No. 11621131001). The work of S. F. was supported by the US Department of Energy (Grant No. DE-FG02-95ER40934). The work of P.C is supported by the U.S. Department of Energy, Office of Science, Office of Nuclear Physics, under Grant No. DE-FG02-94ER40848.

- 
- [1] A. Bohr and B. R. Mottelson, *Nuclear Structure* (Benjamin, New York, 1975), Vol.II.
- [2] L. D. Landau and E. M. Lifshitz, *Course of Theoretical Physics*, Mechanics, Vol. 1 (Pergamon Press, London, 1960)
- [3] S. W. Ødegard et al., Phys. Rev. Lett. **86**, 5866 (2001).
- [4] D. R. Jensen et al., Phys. Rev. Lett. **89**, 142503 (2002).
- [5] P. Brinje et al., Eur. Phys. J. **A 24**, 167 (2005).
- [6] G. Schönwaßer et al., Phys. Lett. **B 552**, 9 (2003).
- [7] H. Amro et al., Phys. Lett. **B 553**, 197 (2003).
- [8] D. J. Hartley et al., Phys. Rev. **C 80**, 041304(R) (2009).
- [9] J. Timár et al., Phys. Rev. Lett. **122**, 062501 (2019).
- [10] S. Biswas et al., Eur. Phys. J. **A 55**, 159(2019).
- [11] J. T. Matta et al., Phys. Rev. Lett. **114**, 082501 (2015).
- [12] N. Sensharma et al., Phys. Rev. Lett. **124**, 052501 (2020)
- [13] N. Sensharma et al., Phys. Lett. **B 792**, 170 (2019).
- [14] S. Frauendorf and F. Dönau, Phys. Rev. **C 89**, 014322 (2014).
- [15] <https://www-nds.iaea.org/public/ensdf-pgm/>
- [16] S. Das et al., Nucl. Instrum. Meth. Phys. Res. **A 893**, 138 (2018).
- [17] D. C. Radford, Nucl. Instrum. Meth. Phys. Res. **A 361**, 297 (1995).
- [18] W.F. Mueller et al., Phys. Rev. **C 59**, 2009 (1999).
- [19] L. T. Song et al., Phys. Rev. **C 71**, 017302 (2005).
- [20] A. Krämer-Flecken, et al., Nucl. Instrum. Methods **A 275**, 333 (1989).
- [21] K. Starosta, et al., Nucl. Instrum. Methods **A 423**, 16 (1999).
- [22] C. Droste, et al., Nucl. Instrum. Methods **A 378**, 518 (1996).
- [23] R. Banik et al., Phys. Rev. **C 101**, 044306 (2020).
- [24] S. Nandi et al., Phys. Rev. **C 99**, 054312 (2019).
- [25] I. Hamamoto, Phys. Rev. **C 65**, 044305 (2002).
- [26] W. X. Shi and Q. B. Chen, Chin. Phys. **C 39**, 054105 (2015).
- [27] E. Streck, Q. B. Chen, N. Kaiser, and U.-G. Meißner, Phys. Rev. **C 98**, 044314 (2018).

- [28] Q. B. Chen, S. Frauendorf, and C. M. Petrache, Phys. Rev. C **100**, 061301(R) (2019).
- [29] *Relativistic Density Functional for Nuclear Structure*, edited by J. Meng International Review of Nuclear Physics Vol. 10 (World Scientific, Singapore, 2016).
- [30] J. Meng, J. Pengi, S.Q. Zhang, S-G. Zhou, Phys. Rev. C **73**, 037303 (2006).
- [31] P.W. Zhao, Z. P. Li, J. M. Yao, and J. Meng, Phys. Rev. C **82**, 054319 (2010).
- [32] P. Joshi et al., Phys. Rev. C **66**, 044306 (2002).
- [33] S. Frauendorf and F. Dönau, Phys. Rev. C **92**, 064306 (2015).
- [34] A.D. Ayangekaa et al., Phys. Rev. Lett. **110**, 172504 (2013).
- [35] T. Roy et al., Phys. Lett. **B 782**, 768 (2018).